nature communications

Article

https://doi.org/10.1038/s41467-025-62204-z

P-stereogenic centre via Pd/Cu-bimetallic catalytic selective phosphinylation of allenylic acetates

Received: 5 March 2025

Accepted: 14 July 2025

Published online: 26 July 2025

Check for updates

Gen Li[1], Shichao Hong[2], Xuechen Li[1], Wenhao Zhao[1], Chaobo Ye[1], Yi Yu[1], Huajie Jiang[1], Jie Yu[1], Xue Zhang[3] ✉, Shengming Ma[2,3] ✉ & Qiankun Li[1] ✉

P-stereogenic organophosphorus compounds are a class of highly important compounds due to their potentials in asymmetric catalysis both as ligands or catalysts and medicinal chemistry. Herein, we report an efficient protocol under bimetallic catalysis of Pd/Cu for highly regio-, *E*- and enantioselective phosphinylation of allenylic acetates with racemic secondary phosphine oxides forming a wide range of versatile P-stereogenic 1,3-dienyl phosphine oxides with 86–95% ee. The regioselectivity is unique as compared to the traditional catalytic enantioselective allenylations.

Control of selectivity is an ever-lasting objective for the precise synthesis of covalent molecules in organic chemistry and medicinal chemistry. Allenes, due to their unique structure, exhibit intriguing and diverse reactivity patterns, thereby substantial efforts have been devoted to the selective transformation of allenes[1–4]. The Pd-catalyzed dynamic kinetic asymmetric transformation of racemic allenylic derivatives has emerged as a promising tool for the construction of axial chirality of allene with the efforts from Imada, Hayashi, Hamada, Trost, Ma, Zhang, and Shao, etc. with C- or N-nucleophiles (Fig. 1a)[5–21]. Triggered by the pivotal role of P-stereogenic organophosphorus compounds in asymmetric catalysis and medicinal chemistry[22–24], we aimed to investigate the possible synthesis of P-stereogenic organophosphorus compounds via phosphinylation of allenylic esters with racemic secondary phosphine oxides (SPO) as the P-nucleophile (Fig. 1b). The challenge would be the precise control of the regio- and stereoselectivity to form either 2,3-allenyl phosphine oxides (allene-**1**–**4**) or 1,3-dienyl phosphine oxides (diene-**1**–**4**). The second challenge would be the control of diastereoselectivity of the 2,3-allenyl phosphine oxides referring to the allene axial chirality and the P-central chirality or the *Z*/*E*-selectivity of the C = C bond in the 1,3-diene products. Moreover, the reactivity of the chiral catalyst is another challenge due to the strong coordination ability of the secondary phosphine oxides via tautomerization to the trivalent phosphinous acid, which would competitively bind to the catalytic amount of metal catalyst, thus greatly reducing the catalytic activity[25–27]. Here we have successfully identified a palladium and copper co-catalytic recipe for the asymmetric phosphinylation of allenylic acetates providing P-stereogenic non-traditional 1,3-dienyl phosphine oxides (Fig. 1c). This transformation features a broad substrate scope and mild conditions with high regio-, *E*-, and enantioselectivity. Control studies revealed that CuCl and TMG are crucial for both reactivity and enantioselectivity.

Results

Optimization of reaction conditions

As shown in Table 1, the reaction conditions were optimized with racemic 4-cyclohexylbuta-2,3-dienyl acetate **1a** and racemic methyl(phenyl)phosphine oxide **2a** as the substrates. Initial studies were focused on the evaluation of chiral phosphine ligands (**L1**-**L7**, 12 mol%) with $[Pd(allyl)Cl]_2$ (5 mol%) as the catalyst in the presence of TMG (2.0 equiv) in DCE (0.1 M) at 0 °C for 36 h. The use of *P*,*N*-bidentate ligand **L1** or bidentate phosphine ligand **L2** didn't provide any product. To our surprise, this Pd-catalyzed phosphinylation of allenylic acetates with chiral biaryl bidentate phosphine ligand (**L3**, **L4**, **L5**) has shown exclusive regioselectivity providing the P-stereogenic 1,3-dienyl phosphine oxide **3a** in 17–53% yields, without formation of the traditional axially chiral allenylic phosphine oxide **4a**. However, the product

[1]Department of Applied Chemistry, Anhui Province Engineering Laboratory for Green Pesticide Development and Application, and Anhui Province Key Laboratory of Crop Integrated Pest Management, Anhui Agricultural University, Hefei, China. [2]Research Centre for Molecular Recognition and Synthesis, Department of Chemistry, Fudan University, Shanghai, China. [3]State Key Laboratory of Organometallic Chemistry, Shanghai Institute of Organic Chemistry, University of Chinese Academy of Sciences, Shanghai, China. ✉e-mail: xzhang@sioc.ac.cn; masm@sioc.ac.cn; liqk@ahau.edu.cn

https://doi.org/10.1038/s41467-025-62204-z

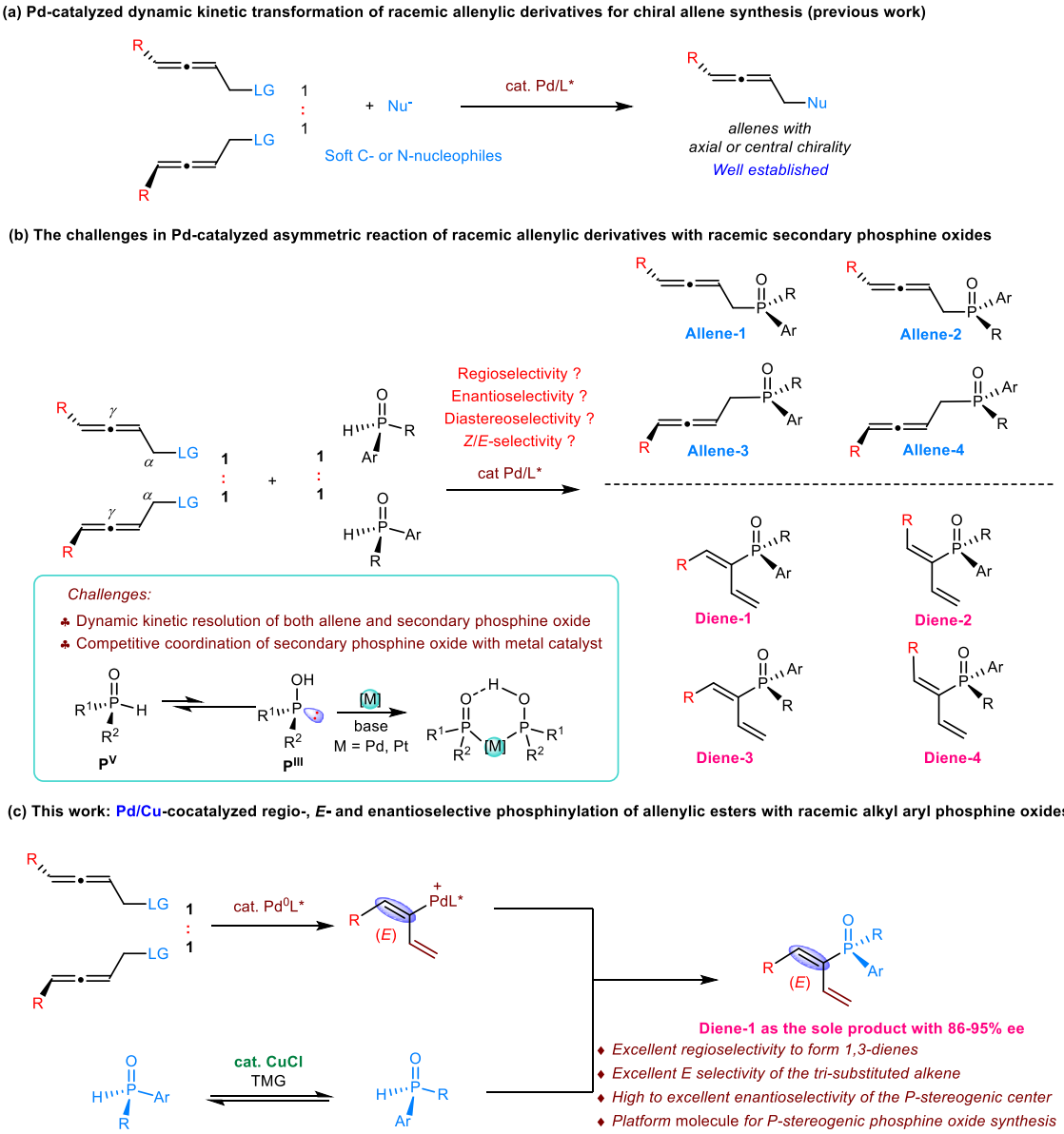

Fig. 1 | Enantioselective reactions of allenylic derivatives with C-/N-nucleophiles and secondary phosphine oxides. a Pd-catalyzed dynamic kinetic transformation of racemic allenylic derivatives for chiral allene synthesis (previous work); **b** The challenges in Pd-catalyzed asymmetric reaction of racemic allenylic derivatives with racemic secondary phosphine oxides; **c** This work: Pd/Cu-cocatalyzed regio-, *E*- and enantioselective phosphinylation of allenylic esters with racemic alkyl aryl phosphine oxides.

was almost racemic (2–6% ee) presumably due to the poisoning effect on the catalyst of the secondary phosphine oxide. Changing the ligand to the MOP **L6** or chiral phosphoramidite **L7** failed to afford either **3a** or **4a**. The reaction was then investigated by adding Lewis acid to improve the reactivity of secondary phosphine oxide[28] with chiral ligand **L5**. Indeed, the inclusion of $FeCl_2$, $CoCl_2$, or $NiCl_2$ (0.5 equiv) improved the yield of **3a** to 40–77%, but did not lead to any improvement of the enantioselectivity (4–7% ee, Table 1, entries 2–4), indicating the asymmetric phosphinylation of allenylic acetates with secondary phosphine oxides is indeed very challenging. Surprisingly, **3a** was afforded in a high enantioselectivity of 90% ee and a moderate yield (48%) when $CuCl_2$ was used (Table 1, entry 5). Encouraged by this result, other Cu^{II} and Cu^{I} salts were then evaluated and CuCl turned out to be the best, providing (R_P,*E*)−**3a** in an excellent isolated yield of 95% and 89% ee with an excellent *E*-selectivity (Table 1, entry 10). It is worth noting that the counter anions of the copper additives have a great effect on the yield probably due to the influence of the counter anions on the Lewis acidity of the metals (Table 1, entries 8–10). A control experiment revealed that the reaction did not proceed without the palladium catalyst (Table 1, entry 11). The additional systematic evaluation of the reaction conditions including solvents and bases were also conducted but in futile (see Supplementary Table 1).

Reaction scope of enantioselective phosphinylation of allenylic acetates

With the optimal conditions in hand (Table 1, entry 10), we next explored the substrate scope of the methodology by examining 4-cyclohexylbuta-2,3-dien-1-yl acetate **1a** with various racemic secondary phosphine oxides **2** (Fig. 2). Firstly, with **Ar** being fixed as the phenyl group, there is a very wide scope for the R^2 group with C1-C3 carbon-chains and alkyl groups with a synthetically versatile methoxy and C = C bonds: the products (R_P,*E*)-**3a**–**3f** were all formed with 80–98% yields and 87–90% ee. Furthermore, benzyl groups with diverse substitutes on the aryl group were also identified to be suitable R^2 for this

https://doi.org/10.1038/s41467-025-62204-z

Table 1 | Optimization studies for enantioselective phosphinylation of allenylic acetates

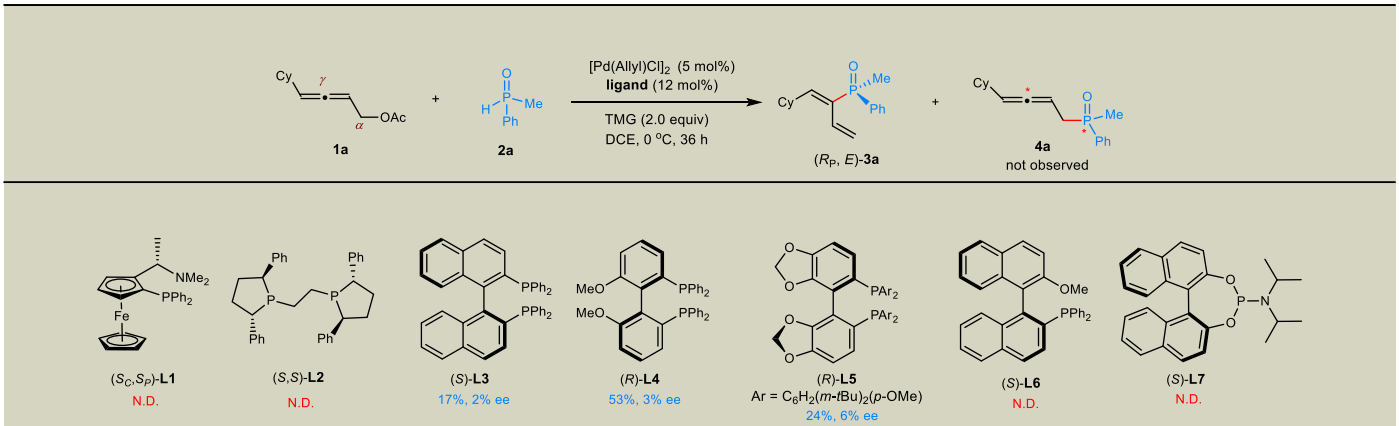

entry[a]	additive	yield (%)	ee (%)
1	-	24	6
2	$FeCl_2$	77	4
3	$CoCl_2$	44	7
4	$NiCl_2$	40	7
5	$CuCl_2$	48	90
6	$CuBr_2$	40	86
7	$Cu(OAc)_2$	65	84
8	CuI	46	88
9	CuBr	64	91
10	CuCl	>99 (95)	89
11[b]	CuCl	N.D.	N.D.

Reaction conditions: **1a** (0.20 mmol), **2a** (2.0 equiv), $[Pd(Allyl)Cl]_2$ (5 mol%), ligand (12 mol%), additives (0 or 0.5 equiv), TMG (2.0 equiv), and DCE (2.0 mL) at 0 °C for 36 h. The yield was determined by ^1H NMR analysis of the reaction mixture with mesitylene as the internal standard, and the ee value was determined by chiral HPLC analysis. N.D. = not detected. TMG = Tetramethylguanidine. [a] with (*R*)-**L5** as the chiral ligand. [b] the catalyst $[Pd(Allyl)Cl]_2$ was omitted.

enantioselective phosphinylation reaction, affording the desired products (R_P,*E*)-**3g**–**3m** in 70–91% yields and 92–95% ee. The secondary phosphine oxides with a variety of alkyl substituents at the para, meta, or ortho position of the aryl group (**Ar**) worked, affording the corresponding products (R_P,*E*)-**3n**–**3t** in 63–97% yields with 86–94% ee. In addition, the *para*-Ph substituted product (R_P,*E*)-**3u** was afforded in 71% yield and 93% ee. Introduction of etheric *meta*- or *para*-C – O bond to the aromatic ring of secondary phosphine oxides led to the formation of (R_P,*E*)-**3v**–**3y** in high yields and high enantioselectivities. Electron-withdrawing group such as F, Cl, or CF_3 in the para position of aryl phosphine oxide was well tolerated delivering (R_P,*E*)-**3z**–**3ab** in 51–82% yields and 86–92% ee. The naphthalene and benzothiophene were also applicable, and the corresponding product (R_P,*E*)-**3ac**–**3ad** were isolated in 76-80% yields with 91% ee. The absolute configuration of products has been successfully established with the single crystal X-ray diffraction analysis of (R_P,*E*)-**3g** (CCDC 2325110).

We next sought to examine the scope of the allenylic acetates **1** with secondary phosphine oxide **2g** (Fig. 2). The isopropyl substituted allenylic acetate delivered the desired (R_P,*E*)-**3ae** in 81% yield and 95% ee. Tetrahydropyran and piperidine were also compatible affording (R_P,*E*)-**3af**–**3ag** in 70–75% yields and 95% ee. It is worth noting that even the strained rings such as cyclopropane and cyclobutane survived and provided (R_P,*E*)-**3ai** and (R_P,*E*)-**3aj** in 92% ee. Furthermore, allenylic acetates bearing a linear C6 alkyl chain at the 4-postion also worked to afford the P-stereogenic product (R_P,*E*)-**3ak** in 81% yield with 90% ee. A variety of functional groups such as chloro, bromo, phenyl, phthalylimide, and alkenyl could be introduced to the primary alkyl chain giving the products (R_P,*E*)-**3al**–**3aq** in 87–91% ee. Moreover, Ph-substituted allenylic acetate was also compatible furnishing the corresponding product (R_P,*E*)-**3ar** in moderate yield with 86% ee.

Synthetic utility

To elucidate the synthetic potential of this method, further transformations of the P-stereogenic products were investigated (Fig. 3). Initially, the reaction of allenylic acetate **1a** with **2g** was successfully scaled up to 5.0 mmol scale, affording the corresponding P-stereogenic phosphine oxide (R_P,*E*)-**3g** with a comparable yield and enantioselectivity (1.4812 g, 85% yield and 92% ee, Fig. 3a). Then oxidative Heck reaction of (R_P,*E*)-**3g** with 4-methylbenzeneboronic acid could provide P-stereogenic 1,3-dienyl phosphine oxide (R_P,*E*,*E*)-**4** in 63% yield[29]. In addition, reduction of (R_P,*E*)-**3a** was realized to afford the phosphine-BH_3 adduct **5** in 60% yield and 90% ee (Fig. 3b). Furthermore, the P-stereogenic cyclic products (R_P,*E*)-**6** and (R_P,*E*)-**7** could be furnished without the erosion of ee via the intramolecular olefin metathesis reaction under the catalysis of the Grubbs (II) catalyst (Fig. 3c)[30].

Mechanism study and DFT calculation

To unveil the mechanistic nature of this Pd-catalyzed phosphinylation of allenylic acetates, we first examined the impact of the amount of CuCl to unveil the crucial role of CuCl (Fig. 4a). When the amount of CuCl was reduced from 50 mol% to 20 mol%, the yield of (R_P,*E*)-**3a** dropped dramatically from 99% to 59% with a slightly decreased enantioselectivity (89% ee vs. 84% ee). Further reducing the amount of CuCl to 10 mol% resulted both in a sharply decreased yield and enantioselectivity (25% yield and 42% ee). The enantioselectivity of the product (R_P,*E*)-**3a** was merely 6% ee when CuCl was omitted. Further increasing of the amount of CuCl to 1.0 equivalent resulted in a lower yield and same ee. These results strongly suggest a critical role of CuCl for control of the enatioselectivity and the reactivity of secondary phosphine oxide. The Pd-catalyzed phosphinylation of racemic substrate **1a** was also performed at partial conversion, and the unreacted

https://doi.org/10.1038/s41467-025-62204-z

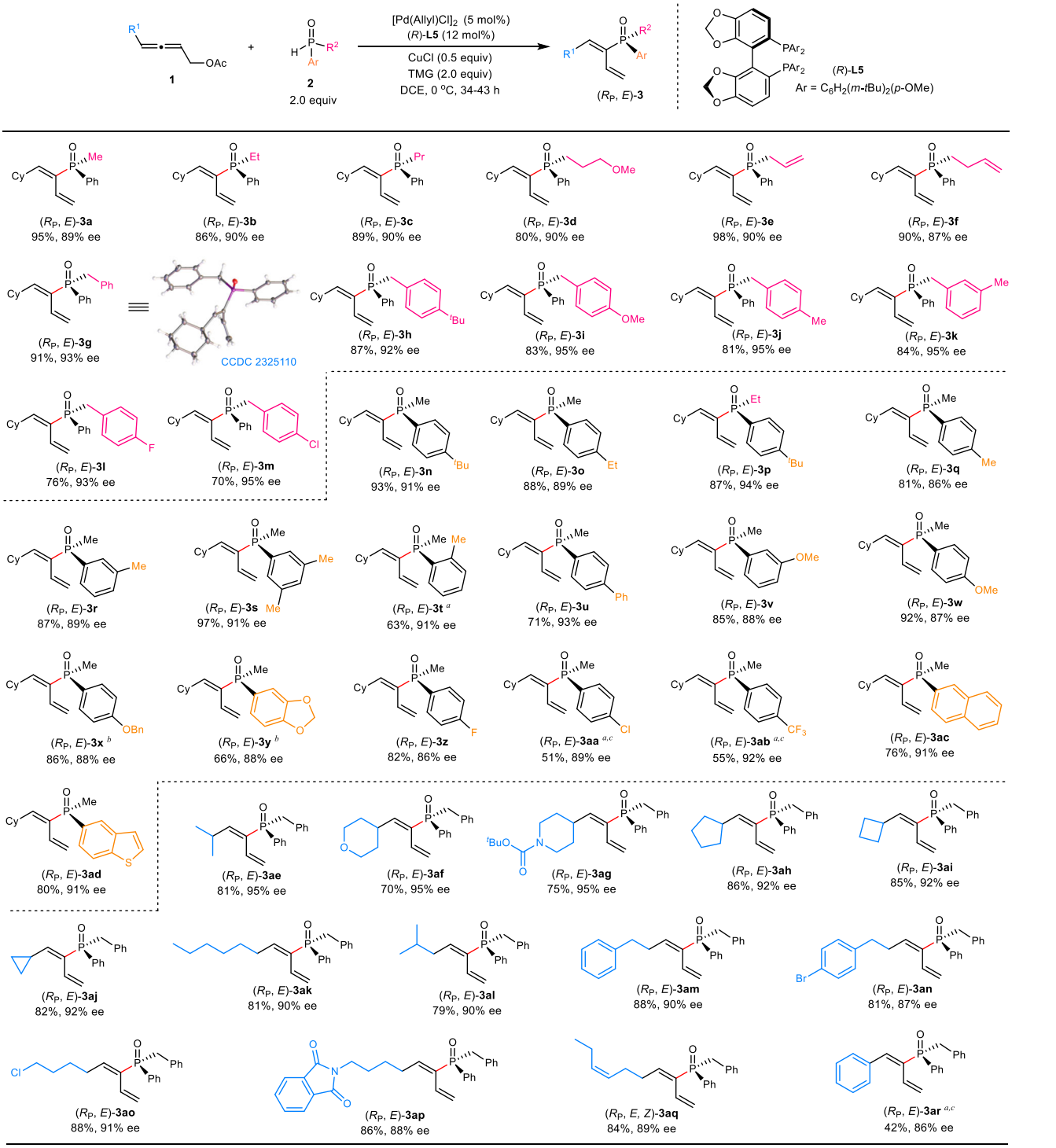

Fig. 2 | Substrate scope of the enantioselective phosphinylation of allenylic acetates. Reaction conditions: **1** (0.20 mmol), **2** (2.0 equiv), $[Pd(Allyl)Cl]_2$ (5 mol%), (*R*)-**L5** (12 mol%), CuCl (0.5 equiv), TMG (2.0 equiv), and DCE (2.0 mL) at 0 °C for 34-43 h. The ee value was determined by chiral HPLC analysis. [a] the reaction was conducted at 10 °C for 60 h; [b] the reaction was conducted at −10 °C; [c] the reaction was conducted with $CHCl_3$ as the solvent. TMG = Tetramethylguanidine.

allenylic acetate **1a** was recovered in only 7% ee (Fig. 4b). Furthermore, the reaction of **1a** with **2a** in the presence of enantiomeric ligand of (*S*)-**L5** under the optimized conditions afforded the enantiomer (S_P,*E*)-**3a** in 82% yield with 90% ee, indicating that the absolute configuration of the P-stereogenic center has been dictated by that of the ligand and the *E*-selectivity has nothing to do with the absolute configuration of the ligand (Fig. 4c). In addition, we prepared the enantioenriched (S_P)-**2a**[31] and subjected it to the standard reaction conditions with (*R*)-**L5** as the ligand and the reaction led to the perfect matched formation of the product (R_P, *E*)-**3a** with a higher enantioselectivity of 95% ee (Fig. 4d, Eq. 1) while the same reaction of (S_P)-**2a** with (*S*)-**L5** as the ligand (to mimic the reaction of (R_P)-**2a** with (*R*)-**L5** as we could not get the (R_P)-**2a** in high ee), the enantiomer (S_P,*E*)-**3a** was obtained in comparable yield with a much lower enantioselectivity of 81% ee (Fig. 4d, Eq. 2). Interestingly, when the reaction of **1a** with (S_P)-**2a** (90% ee) was conducted without CuCl, the same product (R_P,*E*)-**3a** was afforded in a much lower yields of 29-32% with 90% ee and 91% ee with (*R*)-**L5** or (*S*)-**L5** as the ligand (Fig. 4d, Eq. 3 and 4). Then we subjected (S_P)-**2a** to the reaction

https://doi.org/10.1038/s41467-025-62204-z

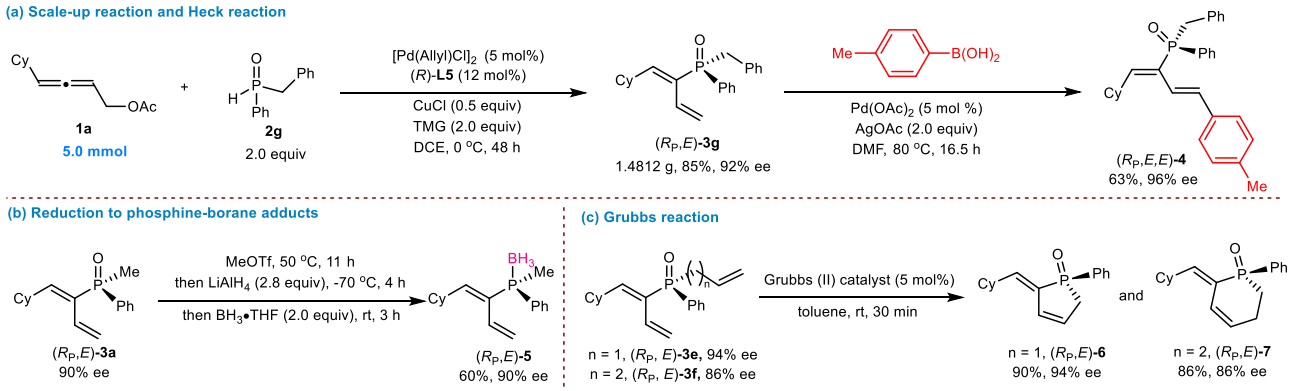

Fig. 3 | Scale-up synthesis and derivatizations. a Scale-up reaction and Heck reaction; **b** Reduction to phosphine-borane adducts; **c** Grubbs reaction.

with various conditions (Fig. 4e): No racemization was observed in 12 h under the conditions with either TMG or the Pd catalyst, while a very low racemization was observed in the presence of CuCl or the Pd/TMG. However, (S_P)-**2a** was almost completely racemized within 2 h in the presence of both CuCl and TMG, implying that CuCl and TMG worked together for the rapid racemization of secondary phosphine oxides. Those results indicated that this Pd-catalyzed enantioselective phosphinylation reaction should be mostly a dynamic kinetic transformation process.

Based on these data we proposed the catalytic cycle depicted in Fig. 4f. The oxidative addition of PdL* with **1a** would generate the η^1-1,3-dienyl-Pd species *E*-**A**[32]. (S_P)-**2a** would replace OAc^- to coodinate with Pd atom in *E*-**A**, yielding complex *E*-**B**. Deprotonation of *E*-**B** with TMG leads to the formation of intermediate *E*-**C**. The nucleophilic substitution of phosphine on the palladium produces the phosphoryl palladium intermediate *E*-**D**, which is followed by reductive elimination to produce the final product (R_P,*E*)-**3a**. At the meantime, the slowly reacting SPO (R_P)-**2a** would undergo rapid racemization to form (S_P)-**2a** by pyramidal inversion[33,34] in the presence of CuCl and TMG.

To further clarify the reaction mechanism as well as the critical role played by CuCl, density functional theory (DFT) calculations were carried out to probe the reaction between **1a** and **2a**, utilizing (*R*)-**L5** as the ligand (for details, see Supplementary Information). As illustrated in Fig. 5a, the formation of complex **Int1**, which was selected as the free energy reference, involves the coordination of Pd atom with the $C^2=C^3$ double bond in (*R*)-**1a**. The subsequent oxidative addition proceeds irreversibly via transition state **TS1** with a free energy barrier of 5.9 kcal/mol, providing the η^1-1,3-dienyl-Pd intermediate **Int2**. The enantiomer (*S*)-**1a** could also undergo oxidative addition to produce **Int2**, with a slightly higher energy barrier of 8.1 kcal/mol via **TS1'**. (S_P)-**2a** participates in the reaction through ligand exchange with OAc^- in **Int2**, providing **Int3_1** with an endergonicity of 13.9 kcal/mol. The subsequent deprotonation of **Int3_1** by TMG proceeds through **TS2_1** with an activation barrier of 27.7 kcal/mol (**TS2_1** relative to **Int2**) to yield **Int4_1**, simultaneously facilitating the conversion of pentavalent to trivalent phosphine. On the other hand, the involvement of CuCl would greatly facilitate the deprotonation step by the coordination of copper with the oxygen of SPO, reducing the free energy barrier to only 10.2 kcal/mol. Notably, CuCl also stabilizes both intermediates **Int3** and **Int4**, and a Gibbs free energy change of −4.2 kcal/mol indicates that this deprotonation step is irreversible. Subsequently, the nucleophilic substitution of phosphine on the palladium center in **Int4** requires a free energy of only 6.2 kcal/mol (**TS3**), resulting in the formation of a phosphoryl palladium intermediate **Int5**, which is exergonic by 12.0 kcal/mol (relative to **Int4**). The reductive elimination of **Int5** produces the final product dienyl phosphine oxide (R_P,*E*)-**3a**, which features an energy barrier of 22.0 kcal/mol (**TS4**) and is the rate limiting step of the whole process.

Furthermore, computational investigations were conducted to elucidate the regioselectivity of the reaction. Due to the facile σ-π-σ tautomerization, η^1-1,3-dienyl-Pd intermediate **Int4** could convert to η^1-allenyl-Pd intermediate **Int7** via the π-allyl Pd intermediate **Int6**. The final (R_P,*E*)-**3a** product may also be achieved through the nucleophilic attack of the phosphine atom on the central carbon C^1 of allene in **Int7** via **TS5**, a pathway rendered less favorable by 11.1 kcal/mol in comparison to **TS4**. The phosphine atom directly attacks the terminal carbon C^3 of allene in **Int4** to yield the allenylic phosphine oxide **4a** via **TS6**. However, owing to the 12.0 kcal/mol higher in free energy of **TS6** compared to **TS4**, no allene products were observed in the experiments. In the Pd-O intermediate **Int4**, the trivalent phosphine can undergo intramolecular nucleophilic attack at three possible sites: the Pd center, the central carbon (C^1), or the terminal carbon (C^3). Natural Population Analysis (NPA) reveals that for the the Pd atom carries positive charge (+0.083), while C^1 and C^3 are negatively charged (−0.190 and −0.381, respectively), strongly favoring nucleophilic attack at the Pd site (Fig. 5b). To further support this, we computed the local electrophilicity index (ω_k), which shows that the Pd center has the highest electrophilicity (0.032 eV), surpassing those of C^1 (0.025 eV) and C^3 (0.024 eV). These findings align with the observed activation barriers: **TS3** (Pd path) is significantly lower in energy than **TS5** (C^1 path, +14.9 kcal/mol) and **TS6** (C^3 path, +15.8 kcal/mol), confirming that the Pd site is the most favorable for nucleophilic attack. Furthermore, the phosphoryl palladium intermediate **Int5** undergoes reductive elimination via two competing pathways: (1) C^1-P bond formation through a 3-membered cyclic **TS4**, or (2) C^3-P bond formation via a 5-membered cyclic **TS7**. The latter pathway is energetically disfavored, with **TS7** exhibiting a 38.9 kcal/mol barrier (16.9 kcal/mol higher than **TS4**). This energy difference originates from greater structural distortion in **TS7**, as evidenced by bond angle comparisons (Fig. 5b): while **TS4** (α = 112.9°, β = 125.4°) shows minimal deviation from **Int5** (α = 115.0°, β = 127.0°), **TS7** (α = 106.0°, β = 123.2°) displays significant angular strain. The enhanced distortion in **TS7** accounts for both its higher energy and the observed regioselectivity for the reductive elimination of **Int5**.

Additionally, computational analyses were undertaken to elucidate the observed enantioselectivity. The deprotonation step of **Int3** to **Int4** is computed to be irreversible and the subsequent nucleophilic substitution and reductive elimination both preserve the enantioselectivity. Thus, the deprotonation step is considered as the enantioselectivity-determining step. The deprotonation transition state **TS2'** for (R_P)-**2a** is disfavored due to an increased Gibbs free energy of 2.7 kcal/mol compared to the transition state **TS2** associated with (S_P)-**2a**, thereby elucidating the enantioselectivity of the reaction (Fig. 5c). The IGMH[35] analysis of **TS2** identifies two stabilizing C−H···π interactions (2.50 Å and 2.79 Å) between SPO (S_P)-**2a** and the PdL*-allyl moieties, which contributed to the stabilization the **TS2** structure. In

https://doi.org/10.1038/s41467-025-62204-z

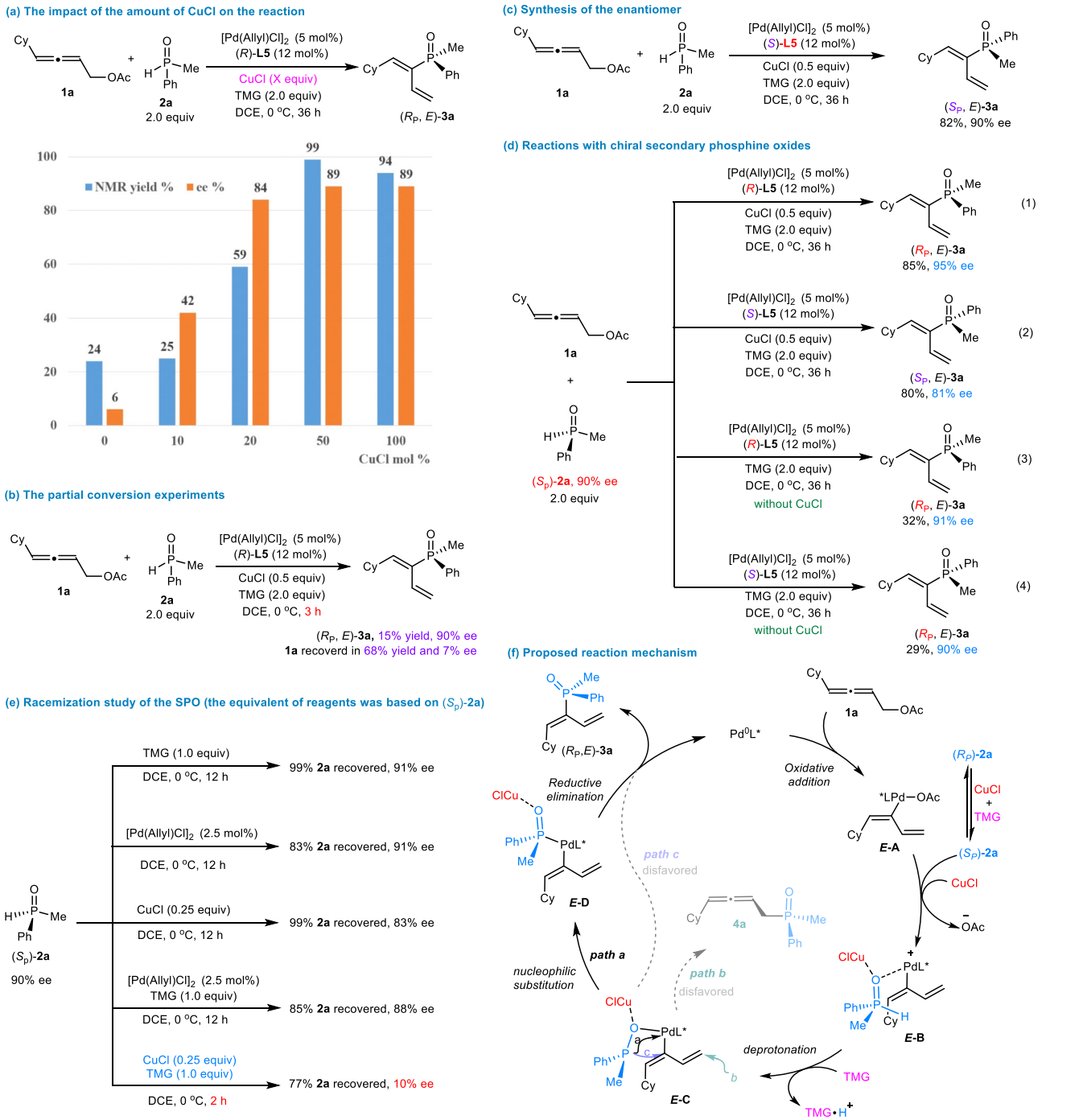

Fig. 4 | Control experiments and proposed reaction mechanism. a The impact of the amount of CuCl on the reaction; **b** The partial conversion experiments; **c** Synthesis of the enantiomer; **d** Reactions with chiral secondary phosphine oxides; **e** Racemization study of the SPO (the equivalent of reagents was based on (S_p)−**2a**); **f** Proposed reaction mechanism.

contrast, **TS2'** lacks comparable non-covalent interactions. Instead, the shortest H···H contact (2.02 Å) between the cyclohexyl and methyl groups indicates significant steric repulsion. The combination of stabilizing C-H···π interactions in **TS2** and destabilizing steric clash in **TS2'** rationalizes the 2.7 kcal/mol energy difference between the two transition states.

Discussion

In this work, we have developed a highly regio-, *E*-, and enantioselective catalytic phosphinylation of allenylic acetates forming a chiral phosphine center within the 1,3-dienyl phosphine oxide skeleton. The roles of CuCl and TMG for rapid racemization of SPO and deprotonation have been unveiled and validated by DFT studies, which also rationalize the origin of the observed regio- and enantiocontrol.

Methods

Materials

Unless otherwise noted, materials were purchased from commercial suppliers and used without further purification. All the solvents were treated according to general methods. Flash column chromatography was performed using 200–300 mesh silica gel. See Supplementary Methods for experimental details.

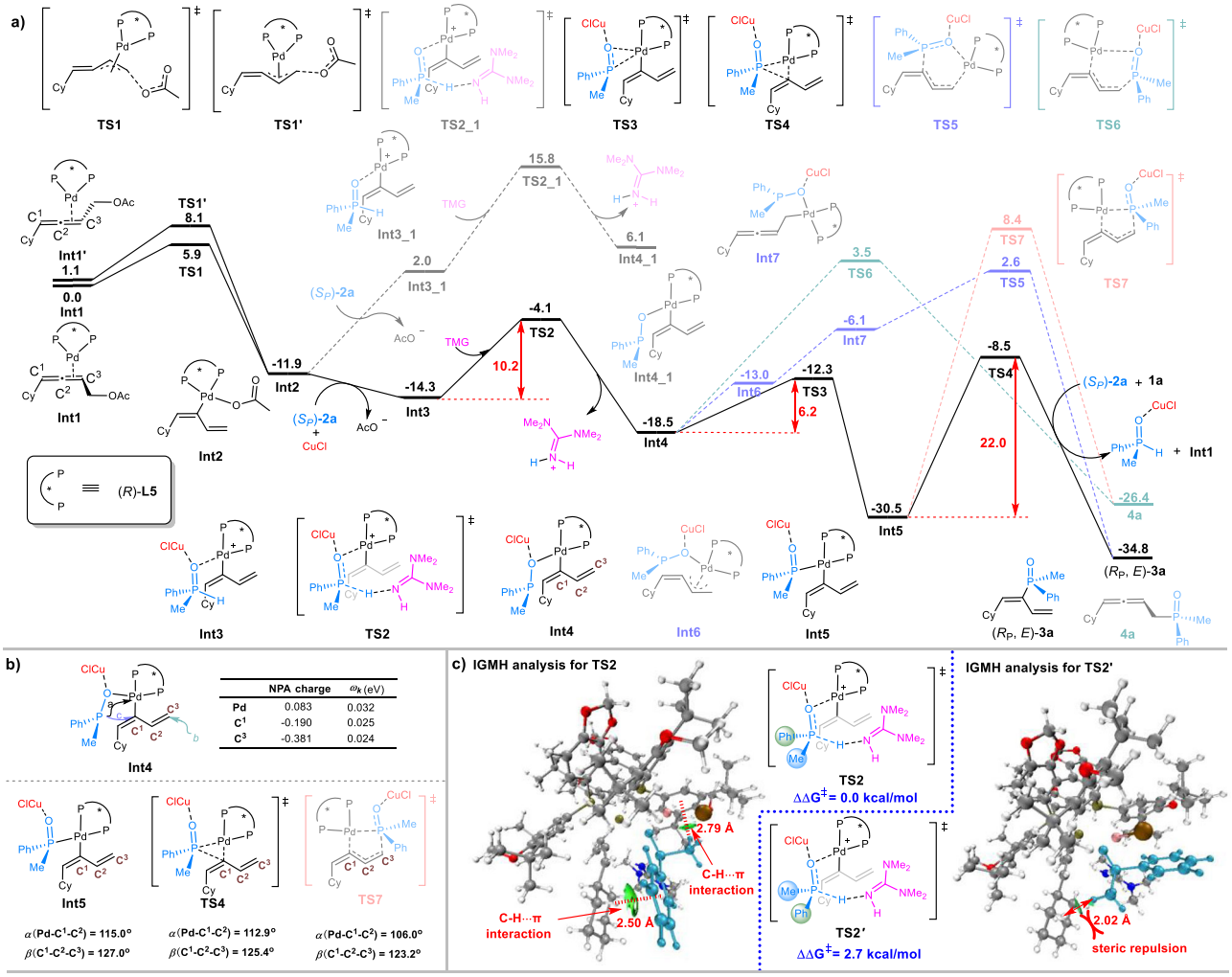

Fig. 5 | Density functional theory (DFT) calculations. a Free energy profiles (ΔG_{sol} in kcal/mol) for the reaction of **1a** and **2a**. **b** The origin of the regioselectivity. **c** The origin of the enantioselectivity.

Procedure for regio- and enantioselective phosphinylation of allenylic acetates. To an oven dried 10 mL Schlenk tube was added CuCl (0.1 mmol, 0.5 equiv), $[Pd(allyl)Cl]_2$ (0.01 mmol, 5 mol%), chiral phosphine ligand (*R*)-**L5** (0.024 mmol, 12 mol%), DCE (2.0 mL), TMG (0.4 mmol, 2.0 equiv), allene **1** (0.2 mmol), and phosphine oxide **2** (0.4 mmol, 2.0 equiv) sequentially under nitrogen. The Schlenk tube was then sealed and stirred for 36 h at 0 °C. The reaction mixture was then filtered through a pad of celite eluenting with CH_2Cl_2/EtOAc (20 mL). The filtrate was concentrated, and the residue was purified by silica gel chromatography to afford the corresponding product.

Data availability

The authors declare that the data supporting the findings of this study are available within the article and its Supplementary Information file. For the experimental procedures, data of NMR and HPLC analysis, see Supplementary Methods and Charts in Supplementary Information file. The X-ray crystallographic coordinates for structures reported in this article have been deposited at the Cambridge Crystallographic Data Center ((*R*P,*E*)-**3g**: CCDC 2325110). These data could be obtained free of charge from The Cambridge Crystallographic Data Center via www.ccdc.cam.ac.uk/data_request/cif. Data supporting the findings of this manuscript are also available from the corresponding author upon request.

References

1. Ma, S. Transition metal-catalyzed/mediated reaction of allenes with a nucleophilic functionality connected to the α-carbon atom. *Acc. Chem. Res.* **36**, 701–712 (2003).
2. Ma, S. Some typical advances in the synthetic applications of allenes. *Chem. Rev.* **105**, 2829–2871 (2005).
3. Blieck, R., Taillefer, M. & Monnier, F. Metal-catalyzed intermolecular hydrofunctionalization of allenes: easy access to allylic structures via the selective formation of C–N, C–C, and C–O bonds. *Chem. Rev.* **120**, 13545–13598 (2020).
4. Pagès, L., Abdine, R. A. A., Monnier, F. & Taillefer, M. Transition metal-catalyzed intermolecular hydroarylation of allenes. *Eur. J. Org. Chem.* **2022**, e20220072 (2022).
5. Ogasawara, M., Ikeda, H., Nagano, T. & Hayashi, T. Palladium-catalyzed asymmetric synthesis of axially chiral allenes: a synergistic effect of dibenzalacetone on high enantioselectivity. *J. Am. Chem. Soc.* **123**, 2089–2090 (2001).
6. Trost, B. M., Fandrick, D. R. & Dinh, D. C. Dynamic kinetic asymmetric allylic alkylations of allenes. *J. Am. Chem. Soc.* **127**, 14186–14187 (2005).
7. Imada, Y., Nishida, M., Kutsuwa, K., Murahashi, S.-I. & Naota, T. Palladium-catalyzed asymmetric amination and imidation of 2,3-allenyl phosphates. *Org. Lett.* **7**, 5837–5839 (2005).

8. Nemoto, T., Kanematsu, M., Tamura, S. & Hamada, Y. Palladium-catalyzed asymmetric allylic alkylation of 2,3-allenyl acetates using a chiral diaminophosphine oxide. *Adv. Synth. Catal.* **351**, 1773–1778 (2009).
9. Wan, B. & Ma, S. Enantioselective decarboxylative amination: synthesis of axially chiral allenyl amines. *Angew. Chem. Int. Ed.* **52**, 441–445 (2013).
10. Song, S., Zhou, J., Fu, C. & Ma, S. Catalytic enantioselective construction of axial chirality in 1,3-disubstituted allenes. *Nat. Commun.* **10**, 507 (2019).
11. Zha, T. et al. Direct catalytic asymmetric and regiodivergent N1- and C3- allenylic alkylation of indoles. *Angew. Chem. Int. Ed.* **62**, e202300844 (2023).
12. Li, Q., Fu, C. & Ma, S. Catalytic asymmetric allenylation of malonates with the generation of central chirality. *Angew. Chem. Int. Ed.* **51**, 11783–11786 (2012).
13. Li, Q., Fu, C. & Ma, S. Palladium-catalyzed asymmetric amination of allenyl phosphates: enantioselective synthesis of allenes with an additional unsaturated unit. *Angew. Chem. Int. Ed.* **53**, 6511–6514 (2014).
14. Liu, H.-C., Hu, Y.-Z., Wang, Z.-F., Tao, H.-Y. & Wang, C.-J. Synergistic Cu/Pd-catalyzed asymmetric alenylic alkylation of azomethine ylides for the construction of α-allene-substituted non-proteinogenic α-amino acids. *Chem. Eur. J.* **25**, 8681–8685 (2019).
15. Dai, J., Duan, X., Zhou, J., Fu, C. & Ma, S. Catalytic enantioselective simultaneous control of axial chirality and central chirality in allenes. *Chin. J. Chem.* **36**, 387–391 (2018).
16. Trost, B. M., Schultz, J. E., Chang, T. & Maduabum, M. R. Chemo-, regio-, diastereo-, and enantioselective palladium allylic alkylation of 1,3-dioxaboroles as synthetic equivalents of α-hydroxyketones. *J. Am. Chem. Soc.* **141**, 9521–9526 (2019).
17. Zhang, J. et al. Enantio- and diastereodivergent construction of 1,3-nonadjacent stereocenters bearing axial and central chirality through synergistic Pd/Cu catalysis. *J. Am. Chem. Soc.* **143**, 12622–12632 (2021).
18. Dai, J. et al. Construction of acyclic all-carbon quaternary stereocenters and 1,3-nonadjacent stereoelements via organo/metal dual catalyzed asymmetric allenylic substitution of aldehydes. *Angew. Chem. Int. Ed.* **62**, e202300756 (2023).
19. Zhang, J. et al. Synergistic Pd/Cu-catalyzed 1,5-double chiral inductions. *J. Am. Chem. Soc.* **146**, 9241–9251 (2024).
20. Gong, B. et al. Enantioselective synthesis of axially chiral alkylidenecycloalkanes via copper-catalyzed functionalization of acyl allenols. *ACS Catal.* **15**, 2351–2358 (2025).
21. Gao, L. et al. Nickel-catalyzed enantioselective synthesis of dienyl sulfoxide. *Angew. Chem. Int. Ed.* **63**, e202317626 (2024).
22. Pradere, U., Garnier-Amblard, E. C., Coats, S. J., Amblard, F. & Schinazi, R. F. Synthesis of nucleoside phosphate and phosphonate prodrugs. *Chem. Rev.* **114**, 9154–9218 (2014).
23. Xu, G., Senanayake, C. H. & Tang, W. P-chiral phosphorus ligands based on a 2,3-dihydrobenzo[*d*][1,3]oxaphosphole motif for asymmetric catalysis. *Acc. Chem. Res.* **52**, 1101–1112 (2019).
24. Imamoto, T. P-Stereogenic phosphorus ligands in asymmetric catalysis. *Chem. Rev.* **124**, 8657–8739 (2024).
25. Ackermann, L. Air- and moisture-stable secondary phosphine oxides as preligands in catalysis. *Synthesis* **2006**, 1557–1571 (2006).
26. Dubrovina, N. V. & Börner, A. Enantioselective catalysis with chiral phosphine oxide preligands. *Angew. Chem. Int. Ed.* **43**, 5883–5886 (2004).
27. Shaikh, T. M., Weng, C.-M. & Hong, F.-E. Secondary phosphine oxides: Versatile ligands in transition metal-catalyzed cross-coupling reactions. *Coord. Chem. Rev.* **256**, 771–803 (2012).
28. Cai, B. et al. Asymmetric hydrophosphinylation of alkynes: facile access to axially chiral styrene-phosphines. *Angew. Chem. Int. Ed.* **62**, e202215820 (2023).
29. Song, E., Park, J., Oh, I.-K., Jung, H. M. & Lee, S. Ligand-free palladium-catalyzed Mizoroki-Heck-type reaction of arylboronic acids and alkenes using silver cation. *Bull. Korean Chem. Soc.* **31**, 1789–1792 (2010).
30. Scholl, M., Ding, S., Lee, C. W. & Grubbs, R. H. Synthesis and activity of a new generation of Ruthenium-based olefin metathesis catalysts coordinated with 1,3-dimesityl-4,5-dihydroimidazol-2-ylidene ligands. *Org. Lett.* **1**, 953–956 (1999).
31. Xu, Q., Zhao, C.-Q. & Han, L.-B. Stereospecific nucleophilic substitution of optically pure H-phosphinates: a general way for the preparation of chiral P-stereogenic phosphine oxides. *J. Am. Chem. Soc.* **130**, 12648–12655 (2008).
32. Ogasawara, M. et al. Synthesis, structure, and reactivity of (1,2,3-η^3-butadien-3-yl) palladium complexes. *Organometallics* **26**, 5025–5029 (2007).
33. Reichl, K. D., Ess, D. H. & Radosevich, A. T. Catalyzing pyramidal inversion: configurational lability of P-stereogenic phosphines via single electron oxidation. *J. Am. Chem. Soc.* **135**, 9354–9357 (2013).
34. Wang, X. et al. Enantioselective synthesis of five to eight-membered P-stereogenic benzo-fused heterocycles via copper-catalyzed dynamic kinetic resolution. *Adv. Synth. Catal.* **366**, 2285–2291 (2024).
35. Lu, T. & Chen, Q. Independent gradient model based on Hirshfeld partition: A new method for visual study of interactions in chemical systems. *J. Comput. Chem.* **43**, 539–555 (2022).

Acknowledgments

We are grateful for financial support from National Natural Science Foundation of China (grant No. 92156022 for J.Y., 22001008 for Q.L.), Anhui Provincial Natural Science Funds (grant No. 2308085Y13 for Q.L.), and Anhui Agricultural University.

Author contributions

Q.L. and S.M. conceived and directed the project. G.L. performed the reactions and control experiments. S.H. and X.Z. performed the DFT calculations. X.L., W.Z., C.Y., and Y.Y. helped with the collection of new compounds and data analysis. H.J. and J.Y. helped to discuss the results and commented on the manuscript. Q.L. wrote the paper with input from all other authors. G.L. and S.H. contributed equally to this work.

Competing interests

The authors declare no competing interests.

Additional information

Supplementary information The online version contains supplementary material available at https://doi.org/10.1038/s41467-025-62204-z.

Correspondence and requests for materials should be addressed to Xue Zhang, Shengming Ma or Qiankun Li.

Peer review information *Nature Communications* thanks the anonymous reviewers for their contribution to the peer review of this work. A peer review file is available.